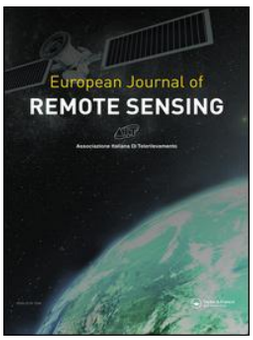

European Journal of Remote Sensing

ISSN: (Print) 2279-7254 (Online) Journal homepage: https://www.tandfonline.com/loi/tejr20

Effectiveness evaluation of the coupled LIDs from the watershed scale based on remote sensing image processing and SWMM simulation

Yan Chen, Ming Tan, Jiahua Wan, Thomas Weise & Zhize Wu

To cite this article: Yan Chen, Ming Tan, Jiahua Wan, Thomas Weise & Zhize Wu (2020): Effectiveness evaluation of the coupled LIDs from the watershed scale based on remote sensing image processing and SWMM simulation, European Journal of Remote Sensing, DOI: 10.1080/22797254.2020.1758962

To link to this article: https://doi.org/10.1080/22797254.2020.1758962

© 2020 The Author(s). Published by Informa UK Limited, trading as Taylor & Francis Group.

Published online: 29 Apr 2020.

Submit your article to this journal

Article views: 235

View related articles

View Crossmark data

Full Terms & Conditions of access and use can be found at
https://www.tandfonline.com/action/journalInformation?journalCode=tejr20

EUROPEAN JOURNAL OF REMOTE SENSING
https://doi.org/10.1080/22797254.2020.1758962

Taylor & Francis
Taylor & Francis Group

OPEN ACCESS Check for updates

Effectiveness evaluation of the coupled LIDs from the watershed scale based on remote sensing image processing and SWMM simulation

Yan Chen[a], Ming Tan[a], Jiahua Wan[b], Thomas Weise[a] and Zhize Wu[a]

[a]School of Artificial Intelligence and Big Data, Hefei University, Hefei, China; [b]School of Information Engineering, Anhui Xinhua University, Hefei, China

ABSTRACT

In this paper, based on remote sensing image processing and SWMM simulation, we evaluate the effectiveness of a coupled LIDs system for the watershed scale. The main content and contributions include: 1) the extraction and classification of historical and recent LULC data (in 1979, 1989, 1999, 2009, 2017) of the study area and an analysis of the characteristics of the LULC change; 2) a watershed-based SWMM applied to the simulation of the runoff and an analysis of the runoff change characteristics; 3) the proposal and design of three coupled LIDs scenarios which treat runoff change as evaluation metric to systematically discuss the effectiveness of LIDs in the watershed. The results show that the combination structure and scale can significantly affect the coupled LIDs effectiveness. A system with multiple LIDs is more effective than one with only single LIDs. With the increase of spatial scale, the effectiveness of the coupled LIDs gradually weakens. Our research enriches the application scale of LIDs and SWMM, and can be beneficial to the construction of the "Sponge City", storm management and urban planning.

ARTICLE HISTORY
Received 8 February 2020
Revised 26 March 2020
Accepted 18 April 2020

KEYWORDS
Low impact development; land use and cover classification; remote sensing; runoff simulation; sponge City; SWMM

Introduction

Low impact development (LID) is the storm management strategy proposed and used firstly in the United States in the 1990s. It mainly applies distributed, source-controlled low impact development devices (or practices, measures) to regulate runoff and non-point source pollution caused by rainfall and urbanization, and to restore the impervious surface area to the state close to the natural hydrological cycle and ecosystem (Eckart et al., 2017). Commonly used LIDs include vegetation swales, rain gardens, rain tanks, permeable paving and retention ponds (Guo et al., 2019). Although LIDs have been widely used in developed countries, due to different developing phases and modes, application and researches in developing countries are still insufficient, and there is a lack of experimental data supporting for the local condition and environment (M. Wang et al., 2018). Since 2014, in response to the urgent issues containing urban flooding, environmental protection and ecological restoration in China (Wang et al., 2004; Xia et al., 2017), "Sponge City" (H. Wang et al., 2018), the innovative urban development mode described from the perspective of integrating storm management and urban planning (He et al., 2019) has been proposed and employed. Implementing wider applications of LIDs, reducing runoff by effectively using LIDs and decreasing the impacts of storms and urbanization on the nature have become the primary goals of "Sponge City" construction (Ding et al., 2019). LID and LIDs begin to enter the fields of the wider application and researches in China.

Compared with LIDs application in developed countries, "Sponge City" not only revolves around storm management, but pays more attention to the regional ecosystem protection and restoration, green space construction, urban microclimate regulation, and sustainable urban planning, which emphasizes comprehensive research and evaluation carried out by combining macro-scale and micro-scale based on the scale-crossed planning theory and methodology (Yu et al., 2015). Currently, most of LIDs effectiveness data come from the micro-scale on-site tests with the single LULC (Ahiablame et al., 2012; Gilbreath et al., 2019; Hou et al., 2019; Noh et al., 2015; Shafique et al., 2018), which are difficult to meet the requirements of the regional planning. Therefore, research on effectiveness of the coupled use of multiple LIDs under the large scale and medium-scale with mixed LULC becomes increasingly urgent. However, in larger regions, due to the limitation of the climate and underlying spatial heterogeneity, conventional LIDs studies based on monitoring experiment and long-term continuous observation significantly increase costs in time and labor (Gu et al., 2019).

With the rapid development of computer science and technology, simulating approaches based on

CONTACT Jiahua Wan jiahwan@163.com School of Information Engineering, Anhui Xinhua University, Hefei, China

© 2020 The Author(s). Published by Informa UK Limited, trading as Taylor & Francis Group.
This is an Open Access article distributed under the terms of the Creative Commons Attribution-NonCommercial License (http://creativecommons.org/licenses/by-nc/4.0/), which permits unrestricted non-commercial use, distribution, and reproduction in any medium, provided the original work is properly cited.

mathematical models and algorithms have been greatly improved on the operation speed and accuracy. Compared with monitoring, simulating can effectively reduce manpower, material resources and time investment for saving costs, and improve application and research efficiency (Ketabchy et al., 2019). At present, LIDs simulation is mainly integrated into the hydrological models in the form of functional components or plug-ins, such as MUSIC, MOUSE, P8-UCM, PURRS, SLAMM, Storm Tac, SWMM, SUSTAIN (Wang et al., 2010), and L-THIA (Xu et al., 2019). In comparison with other models, SWMM (storm water management model) provides more complete LIDs components (Gisvold et al., 2019; Thakali et al., 2018), and supports the distributed, long-term continuous simulation (Campisano et al., 2016), which could improve the results due to climate and underlying spatial heterogeneity. Remote sensing, as one of the considerable means of acquiring extensive earth resources and environmental information, has been widely applied in geography, hydrology, meteorology, mapping, ecology and military reconnaissance on account of its high timeliness, wide area and low costs of global detection and monitoring (Pham et al., 2019). Information extraction based on remote sensing image processing can be beneficial to improve the insufficient field surveys due to the underlying restriction.

Therefore, to enrich the application scale of LIDs and in response to the requirements of the "Sponge City" construction in China, in this paper, we evaluate the effectiveness of a coupled LIDs system from the watershed scale based on remote sensing image processing and SWMM simulation. The main content and contributions include: 1) we classified and extracted the historical and recent LULC data (in 1979, 1989, 1999, 2009, 2017) of the study area, and analyzed the characteristics of LULC change; 2) a watershed-based SWMM had been built and applied to simulate runoff and analyze runoff change characteristics; 3) we proposed and designed three coupled LIDs scenarios which treat runoff change as the evaluation metric to systematically discuss LIDs application in the watershed.

Study area and data

Jinan is one of the first 16 "Sponge City" pilot cities. It is located in eastern China and is the capital of Shandong province. As of 2018, Jinan has 10 districts and 2 counties under its jurisdiction with a total area of 10,244 square kilometers and an urbanization rate of 72.1% (Jinan Municipal People's Government [JMPG], 2019). The terrain of Jinan presents a high elevation in the south and a low elevation in the north. Its average annual temperature is 13.8 degree centigrade and the annual precipitation is 685 mm (Jinan Bureau of Statistics [JBS], 2019). Influenced by elements of the natural topography and landform, clogging of rivers and urban drainage pipes and increased impervious surface caused by the rapid non-matched urbanization, Jinan is encountering acute water risks such as urban waterlogging, non-point source pollution and water ecological degeneration (Y. Zhao et al., 2019). The Xiaoqing River is the only outlet river of the core districts of Jinan. It flows through the districts of Huaiyin, Tianqiao Licheng and Zhangqiu of Jinan, then enters the Bohai Sea of China from Yangjiaogou in Weifang city of Shandong province. The total length is 233 km and the drainage area is 10,336 square kilometers. It is the comprehensive utilization river for flooding control, irrigation and shipping (C. Zhao et al., 2019). The upstream watershed of the hydrological station of Huangtaiqiao on the river was chosen as the simulation area which covers 398 square kilometers and eleven tributaries, namely Lashan River, Nantaiping River, Xingji River, Hongxi River, Beitaiping River, Xigongshang River, Donggongshang River, Xiluo River, Dongluo River, Quanfu River and Liuxing River. Figure 1 shows the location, topography and tributaries in the simulation area called Huangtaiqiao watershed.

The data used in the study mainly include meteorological data, hydrological data, soil data, terrain data, remote sensing data, urban planning data, LIDs data and GIS data. Data sources and descriptions are shown in Table 1. The meteorological data contain the observed precipitation and evaporation records. The hydrological data refer to the observed runoff records used for calibration and verification of SWMM and the measured rivers geometry (parameters and maps). The soil data refer to the soil physical parameters, such as structure, porosity and saturated permeability. Terrain data, i.e. DEM (digital elevation model), are employed to segment the study watershed into several subcatchments to weaken the impact of spatial heterogeneity. DEM with type of SRTM X-SAR and spatial resolution of 30 m was acquired from the German Aerospace Center (abbr. in German as DLR: Deutsches Zentrum für Luft- und Raumfahrt). The remote sensing data consist of Landsat multispectral images (by MSS, TM, and OLI in 1979, 1989, 1999, 2009, 2017, respectively) and high-resolution images from Google Earth, used for LULC classification. The cloud coverage ratios of all images in the simulation area keep less than 1%. Besides the necessary pre-processing, images with spatial resolution of 60 m by the sensor of MSS were resampled to 30 m. The urban planning data mainly include the texts of the master planning of Jinan and the thematic maps used to interpret the historical and recent LULC. The LIDs data consist of the design standards and test results of individual rain tank, rain garden and permeable paving. GIS data are

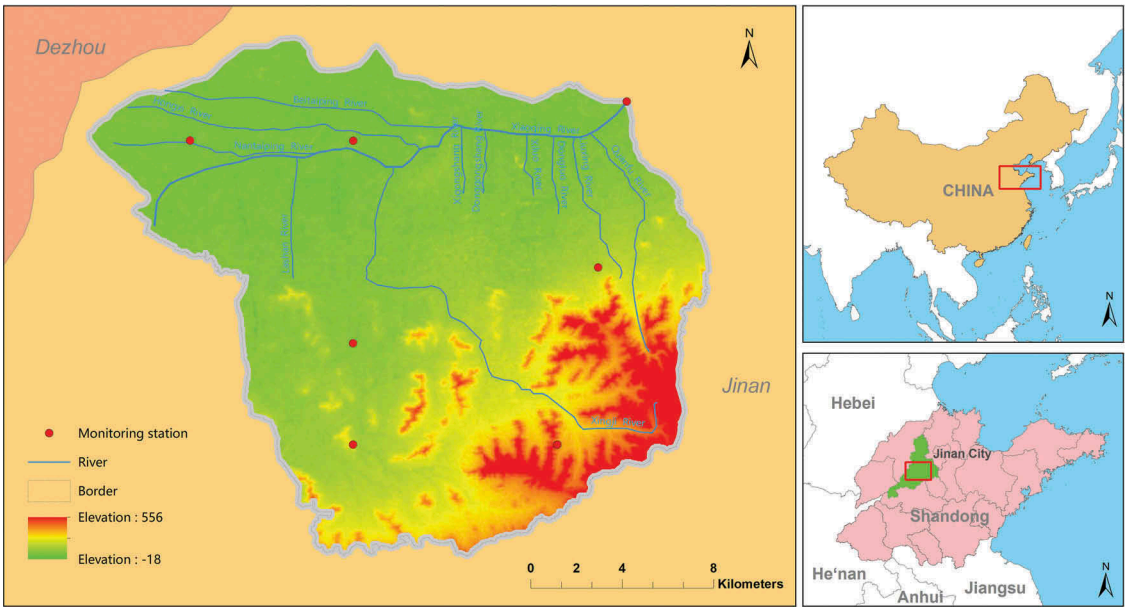

Figure 1. Location map of the study area in Jinan of China.

Table 1. Data used in the study.

Data	Content	Sources
Meteorological data	Observed precipitation and evaporation records	Jinan Hydrological Bureau
Hydrological data	Observed runoff records, measured river geometry	Jinan Hydrological Bureau; Hydrological Yearbook of China
Soil data	Soil physical parameters	Food and Agriculture Organization; Field survey
Terrain data	Elevation (DEM)	German Aerospace Center
Remote sensing data	Landsat images, Google Earth images	United States Geological Survey; Google Earth
Urban planning data	The texts and maps of master planning of Jinan etc.	Jinan Planning Bureau
LIDs data	Designation standards etc.	Jinan Planning Bureau; Handbook of Sponge City
GIS data	Administrative maps, thematic maps etc.	National Geomatics Center of China
Other data	Socio-economic data etc.	Statistical Yearbook of China

mainly applied for location description and mapping, e.g., administrative map and thematic maps. The socio-economic data of the study area were collected from the local statistical yearbooks.

Methodology

The technical route of the study is shown in Figure 2. In this study, the quantified runoff changes before and after the deployment of the combined LIDs are used as the basic evaluation metric. The input data of SWMM cover the topographic, meteorological, soil, and imperviousness data. Most of them were acquired based on the available observation data and field surveys. Generally, the imperviousness measuring the quantity of impervious surface area can be determined from the regional statistics of LULC (Tuomela et al., 2018). Therefore, we firstly use an image classification algorithm, with the assistance of urban planning data, to interpret remote sensing images for extracting LULC of the study area. To better understand the urbanization effect of the study area, we also analyze the characteristics of LULC change based on the classification results. The Non-linear reservoir model integrated into SWMM is applied to simulate runoff with the aid of hydrological data for calibration and verification. According to LIDs data and urban planning data, the coupled LIDs system consisting of rain tank, rain garden and permeable paving has been proposed and designed, which is conceptualized in three scenarios. These scenarios are led into the rectified SWMM for modeling and evaluating the performance of their runoff regulating, respectively. As mentioned above, the crucial procedures of the research involve LULC classification, runoff simulation and scenarios design and modeling of the coupled LIDs. Therefore, in the following sections, we summarized the relevant algorithms, models and processes employed in the study.

Neural network model

An neural network model is a non-linear model with one or more layers of neuron structure developed on the basis of the neuron model (Fu et al., 2018). It was inspired by the biological model of brain neurons and was first applied to machine learning and computer science (Ghorbanzadeh et al., 2019). In the past few

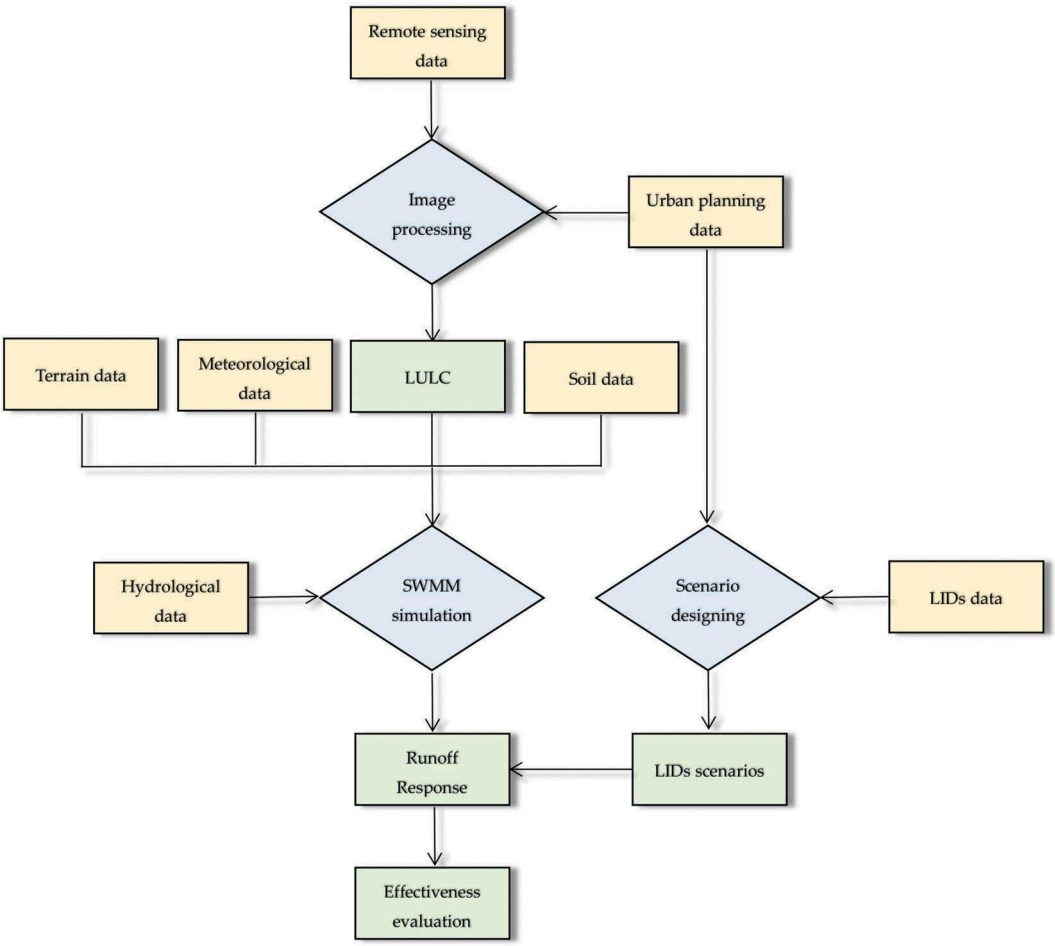

Figure 2. The technical route of the study.

years, neural network model has evolved into a variety of architectures, such as MLP, DBF, CNN, and RNN (Shen, 2018). As the neurons, layers, connection structures and relevant functions of these architectures stay diverse, the components can still be divided into three parts: the input layer, the hidden layer and the output layer. Each layer contains several neurons, for instance, the input layer is generally composed of neurons describing the features of the research objects, and neurons made up the hidden layer are responsible for operating non-linear transformation of the input features, and the output layer receives the non-linear transformation results and performs the related classification. The number of neurons in each layer depends on the research objective.

Currently, neural network models for remote sensing image classification integrated into remote sensing applications generally consist of one or two hidden layers, and the architecture is shown in Figure 3. Neurons of the input layer refer to spectral bands that characterize the spectral feature of various objects. To assume the spectral feature vector as $\boldsymbol{X}$, then the input layer could be expressed like: $\boldsymbol{X} = (x_1$: band 1, x_2: band 2, x_3: band 3, …, x_n: band n). These low-level features are accumulated based on initial weights, then dropped into the non-linear activation function such as sigmoid, tanh or ReLU (Eckle & Schmidt-Hieber, 2018) to acquire advanced features. To assume the output vector as $\boldsymbol{Y}$, the output layer could be presented as: $\boldsymbol{Y} = (y_1$: class 1, y_2: class 2, y_3: class 3, …, y_m: class m). To notate the model parameters vectors as $\boldsymbol{W}$ and $\boldsymbol{B}$, activation function as g, the mathematical description is generalized in followed Equation (1).

$$\boldsymbol{Y} = g(\boldsymbol{W} \times \boldsymbol{X} + \boldsymbol{B}) \tag{1}$$

These parameters can be automatically estimated based on a training set and relevant functions or algorithms such as the objective function, the optimization function and the back propagation algorithm (Ma et al., 2019). In our research, the used spectral bands focus on visible and near-infrared bands in the input layer, and the classified land cover of the output layer includes urban area and non-urban area. The training set or samples were manually obtained from Google Earth images and urban planning data.

Non-linear reservoir model

The non-linear reservoir model (Oosterbaan, 2019) in SWMM conceptualizes the subcatchment as a rectangle

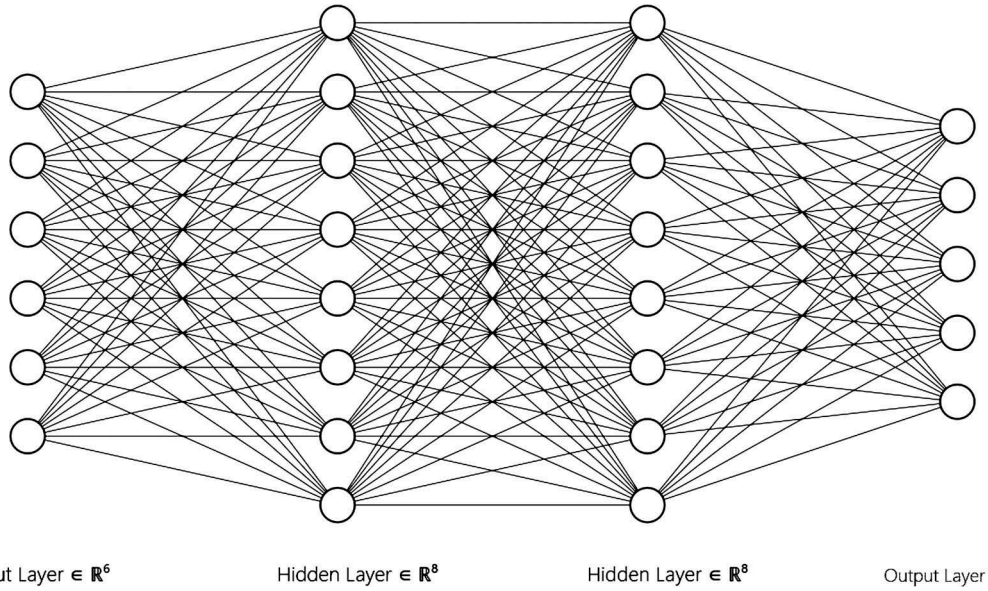

Figure 3. Architecture of neural network model used in remote sensing image classification.

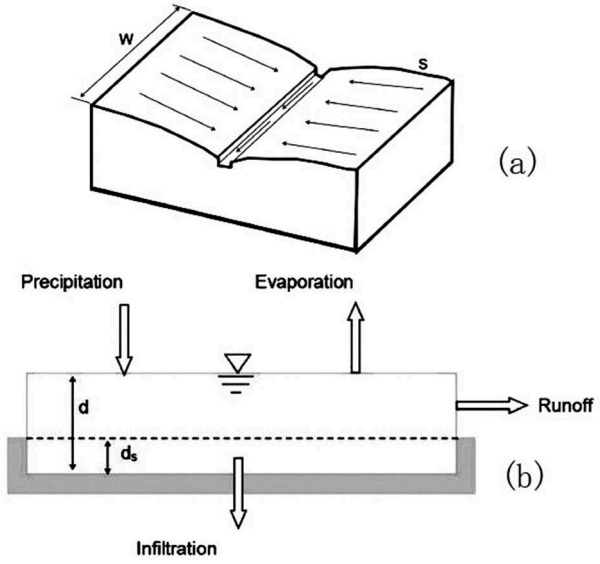

Figure 4. Conceptualized subcatchment and hydrological processes of the non-linear reservoir model (source: US EPA).
US EPA).

with homogeneous slope and width notated by S and W and with only one single outlet as shown in Figure 4 (a). Figure 4(b) depicts the hydrological processes of the subcatchment that the inflow mainly comes from precipitation and makes a loss through evaporation and infiltration. The model assumes that the net rainfall can be accumulated on the surface of the subcatchment with a certain depth notated with d. To deduce the depression storage notated with d_s, the rest can be the runoff. According to the conservation of mass, the depth change of the subcatchment in unit time must be equal to the variation of the outflow quantity as shown in Equation (2). In addition, the model assumes the subcatchment with certain width as a wide non-closed open channel, so the Manning equation or function (Altenau et al., 2019) can be combined with the above-mentioned equation. Equation (3) shows the combined result.

$$q = i - e - f - \frac{\partial d}{\partial t} \tag{2}$$

$$\frac{\partial d}{\partial t} = i - e - f - \frac{K}{n \times A_s} \times W \times \sqrt{S} \times \sqrt[5]{(d - d_s)^3} \tag{3}$$

where S, W, d and d_s have been explicated above, t, i, e, f, q, K, n and A_s are unit time, rainfall rate, evaporation rate, infiltration rate, runoff rate, unit conversion coefficient, The Manning coefficient and the area of subcatchment, respectively.

In our research, the rainfall rate and evaporation rate are from the observed records. The infiltration rate is estimated using the Horton model (Al Maimuri, 2018) based on LULC and the physical parameters of the soil in the study area. The Manning coefficient and depression storage are also determined based on LULC. The slope and area of the subcatchment are calculated in ArcGIS based on a spatial analysis and geometry statistics, respectively. The conceptualized width of the subcatchment is estimated according to the approach proposed in (Jain et al., 2015).

The coupled LIDs scenarios

The simulation of LIDs in SWMM is based on the water quantity balance of the vertical layers conceptualized from the natural layers (Kim & Joo, 2018). Three represented layers known as the surface layer, the soil layer and the storage layer have been demonstrated in Figure 5. The surface layer receives precipitation or runoff generated by its adjacent objects such as roofs, grass and roads, or other LIDs. In addition to surface storage and infiltration to the soil layer or

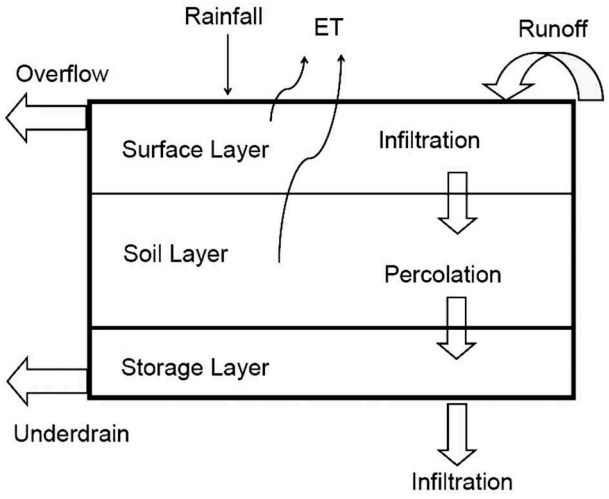

Figure 5. Conceptualized layers for LIDs simulation in SWMM (source: US EPA).

US EPA).

Table 2. Required and optional layers of the frequently used LIDs in SWMM. (source: US EPA).

LIDs	Surface	Pavement	Soil	Storage	Drain	Drainage Mat
Bioretention	X		X	O		
Rain garden	X		X			
Green roof	X		X			X
Permeable paving	X	X	O	X	O	
Infiltration trench	X			X	O	
Rain tank				X	X	
Vegetative swale	X					

storage layer, the excess would enter the urban drainage system or the adjacent area. The soil layer is actually composed of natural or artificial soil to support plants growth and infiltration. Crushed rocks or stones are filled in the storage layer for water detention. In addition, certain independent components or layers rely on certain LIDs. Table 2 shows the required layers (notation: "X") and optional layers (notation: "O") of the frequently used LIDs in SWMM.

As mentioned in section one, current LIDs effectiveness data generated from individual LIDs cannot fulfil the extensional application in the larger scale any more. Hence taking into account the water risks of the study area and the individual LIDs characteristics summarized in (Hao et al., 2019), we choose rain tanks, rain gardens and permeable paving as the basic elements of the coupled LIDs system. Four simulation scenarios consisting of a base scenario and three coupled scenarios have been designed in terms of the runoff path and the runoff portion generated by the impermeable surfaces. The proposed coupled LIDs scenarios follow in Figure 6.

In the base scenario, the runoff generated on roofs, grass or soil surfaces and pavements directly enters the urban drainage system and then eventually converges in the trunk river. As for three coupled LIDs scenarios, scenario 1 assumes that 100% of the roof runoff first enters the rain tanks. The overflowed (or dynamically drained) portion runs into urban pipes since passing on the grass or soil surfaces. Likewise, 50% of the pavement runoff flows into the urban pipes while overflowed from the rain gardens firstly, and the another 50% acted by permeable paving also eventually enters the urban drainage system. Scenario 2 assumes that 50% roof runoff enters the urban drainage system after flowing through the rain gardens. Fifty percent roof runoff enters the rain tanks while the excess enters the urban drainage system since flowing on the surfaces of the grass or soil. One hundred percent pavement runoff enters the urban drainage system after passing from the permeable pavements. Scenario 3 assumes that 50% of roof runoff firstly enters the rain gardens and then is drained to the drainage system. Fifty percent of the roof runoff first enters the rain tanks. The overflowed (or dynamically drained) portion runs into urban pipes since passing on the grass or soil surfaces. The rest process of scenario 3 is similar to the description above and the route in Figure 6. Note that the runoff flowing in the urban pipes eventually runs into the main stream.

Results and analysis

Land use and land cover

Figure 7 shows the classification results of land covers in the key timing-nodes in the study area from 1979 to 2017. The detailed quantitative description of urban area and non-urban area has been listed in Table 3.

The urbanization rate is one of the significant indicators to evaluate urban development (M. Zhao et al., 2019). According to the statistical yearbooks of Jinan, the urbanization rates in the study area from 1979 to 2017 with the step of 10 years were 23.00%, 39.47%, 49.13%, 63.72% and 70.53%, respectively. The changes of urbanization rates are consistent with the land cover obtained by classifying, as shown in Figure 8. During the first 10 years namely from 1979 to 1989, urban area growth compared with other periods maintained the maximum level, because the economy in Jinan was significantly promoted by reforming and opening-up policy of China. Since 1999, the urban area had kept increasing. However, the growth rate started to fall off during 2009, probably the local government had issued relevant laws, regulations and policies to improve the unreasonable growth mode, such as the leap of urban population increase, the non-consistency of urbanization and infrastructure construction, under the extension of the sustainable development. In addition, the establishment and implementation of the new countryside construction during this period might also drive the results. Meanwhile, the results also show that, in order to urbanization rate which depicts the state of urban

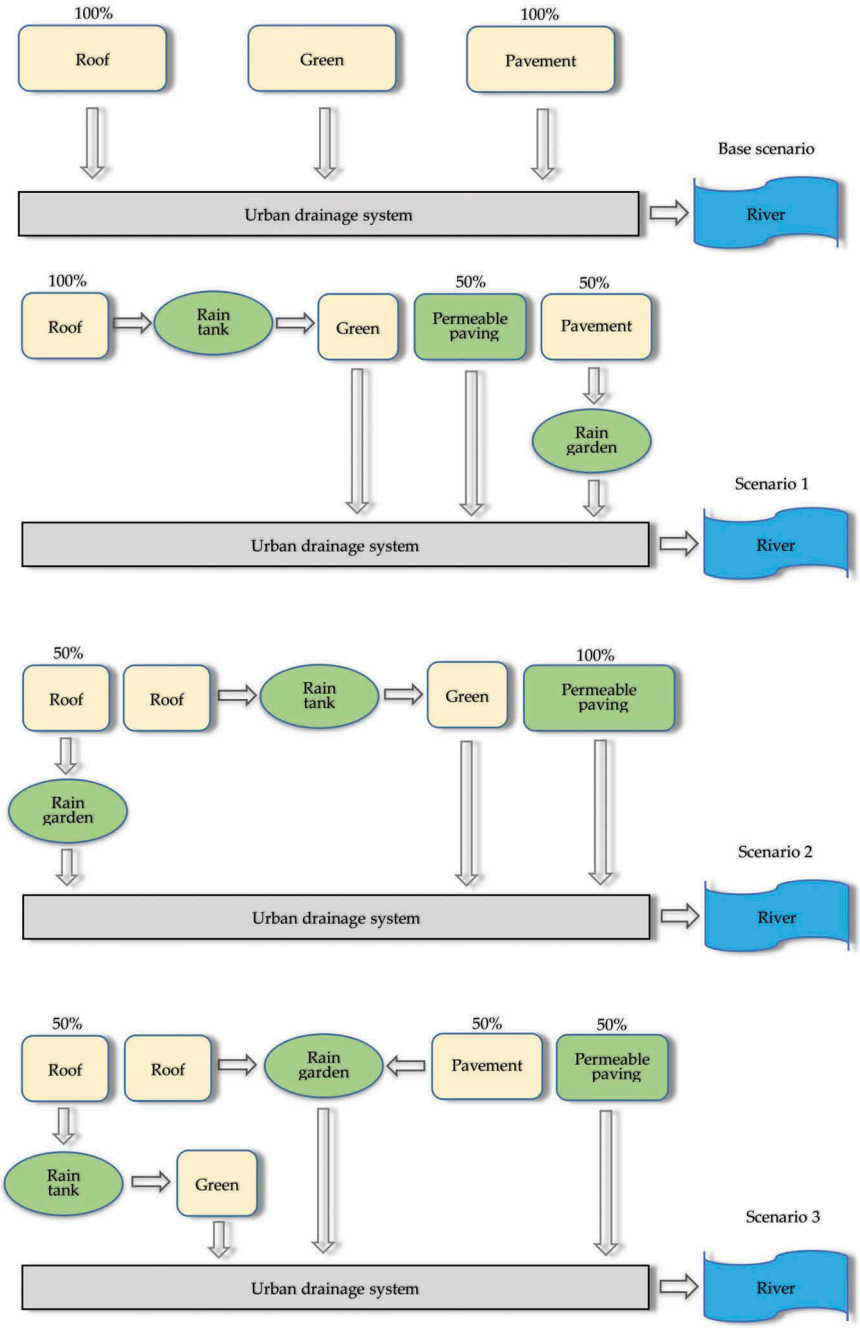

Figure 6. Simulation scenarios proposed in the study.

development from the societal scale, LULC change on the geographical level could also be employed to assess the urban development by taking it as an effective indicator. Based on the results of land cover classification and urban planning data, land use maps in the study area since 1979 were also interpreted as shown in Figure 9. As the land use was only used for parameters estimation such as imperviousness and the Manning coefficient. We do not provide an elaborate analysis here.

Analysis of runoff change

Based on DEM and the actual distribution of the streams, the Huangtaiqiao watershed was divided into 15 subcatchments. In SWMM, the confluence of the stream is treated as the outlet of the whole subcatchment. The trunk stream is segmented into several links by the outlet of the subcatchment. The outlet and link can be represented using the junction object and conduit object of SWMM. In the study, we created 11 junctions and 11 conduits objects shown in Figure 10.

Imperviousness, meteorology and soil parameters were input into the SWMM which simulated the total runoff of the subcatchments and the outfall of the whole watershed shown in Table 4. The variation curves of water yield and urbanization rate in the study area have been drawn in Figure 11. It can be found that the runoff change keeps in accordance with the urbanization rate. Taking into account the

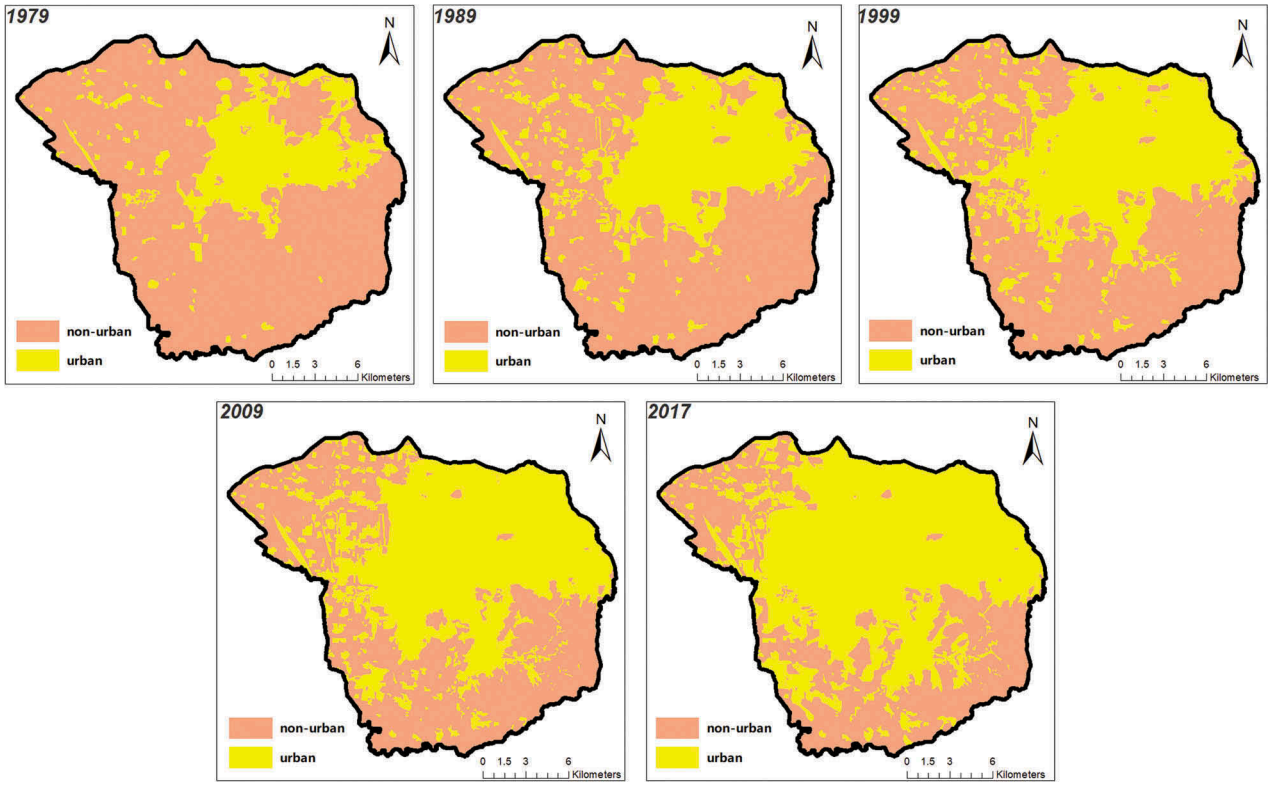

Figure 7. Land cover classification of the study area in 1979, 1989, 1999, 2009 and 2017.

Table 3. Quantitative information of urban area and non-urban area in the study area.

Date	Urban area [km^2]	Non-urban area [km^2]	Urban area percent
1979	88.82	308.59	22%
1989	138.28	259.13	35%
1999	174.91	222.50	44%
2009	212.64	184.77	54%
2017	248.46	148.95	63%

variability of subcatchments, in order to eliminate the influence of various regional underlying surfaces, a runoff coefficient that can characterize the capacity of the rainfall-runoff conversion is applied to replace the total runoff as the evaluation metric. Table 5 and Figure 12 lists and shows the values and changes of runoff coefficients in each subcatchment.

As shown in the forgoing figure, with the development of Jinan, much more impervious surface areas have been rapidly increased. Moreover, due to the difference in local construction intensity, the growth rate also presents variety. From 1979 to 2017, the runoff coefficients in subcatchment S1, S2, S3, S4, S5, S6, S8 and S14 kept continually increasing. The increasing trend in S3 is not significant that indicating low intensity of urban construction in this area. The growth rate of runoff coefficient in subcatchment S4 shows the largest level during 2009 to 2017 compared with the others', which conversely proves the matched

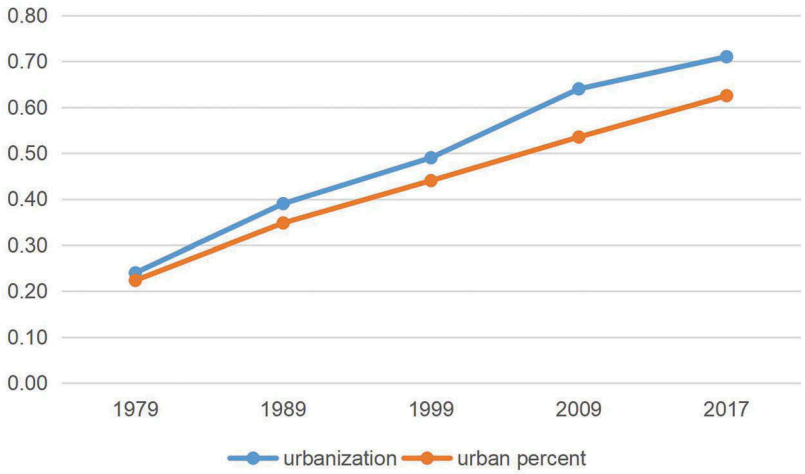

Figure 8. Comparison between urbanization rate and land cover change rate.

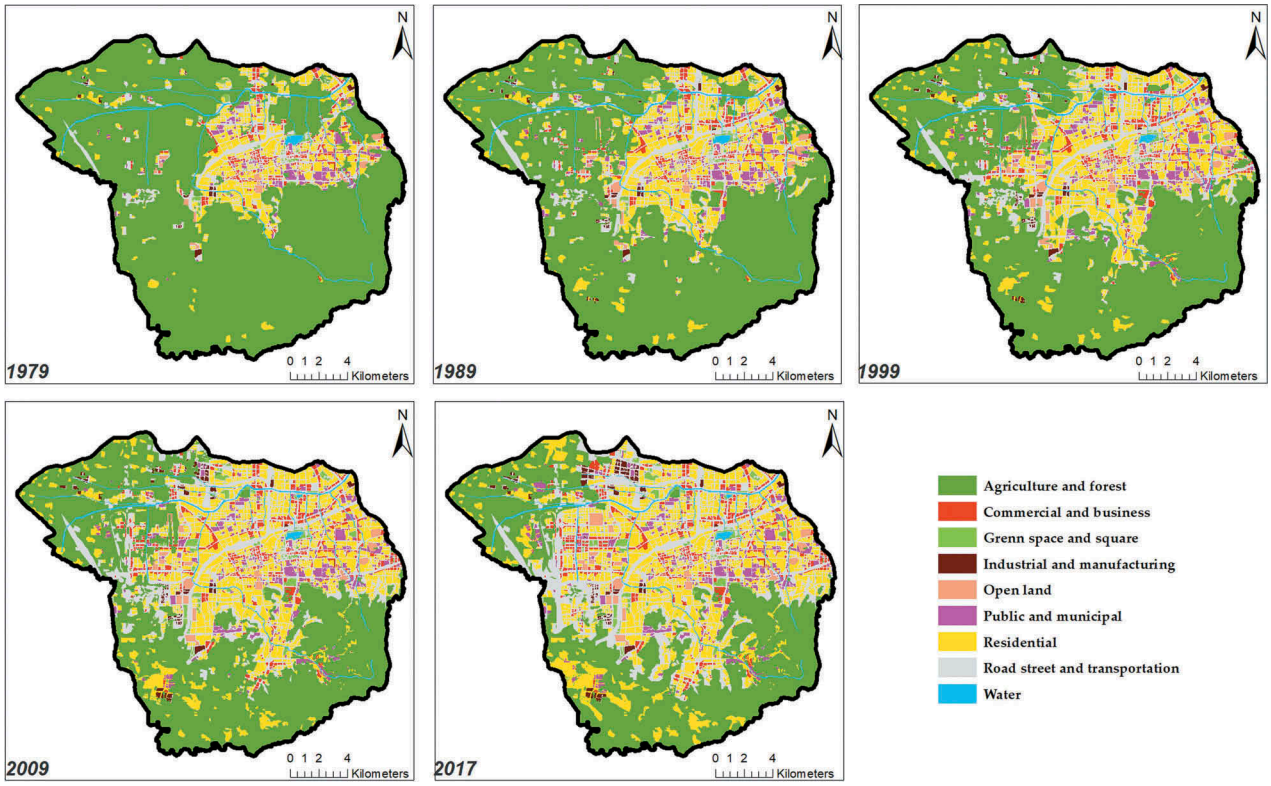

Figure 9. Land use classification of the study area in 1979, 1989, 1999, 2009, 2017.

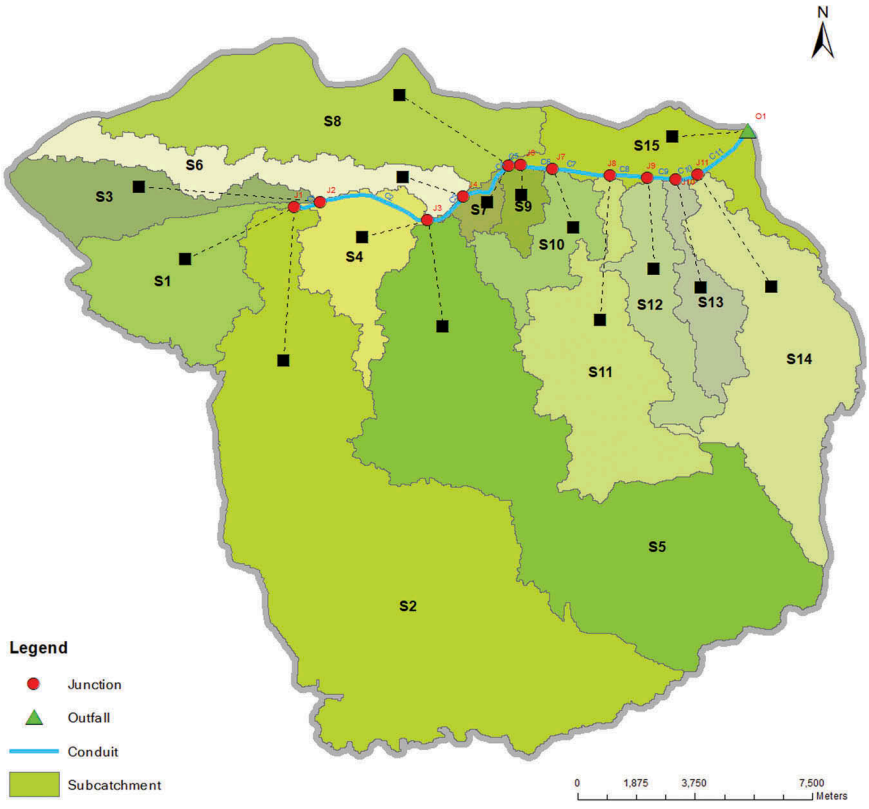

Figure 10. Subcatchment and junction and conduit in the study area.

developed intensity and faster urban development. The runoff coefficients of S7, S9, S10, S11, S12, S13 and S15 all present an increasing trend in the initial phases and then tend to be stable in the later phases, which probably on the one hand because they are located in the urban center leading to higher urbanization level in the beginning. On the other hand, it also shows that the infrastructure construction there is relatively complete since 1989. Note that the runoff coefficients in S9, S10 and S15 present a declining

Table 4. Simulated total runoff of the subcatchments and the whole watershed. (unit: million gal; 1 million gal = 3.7854e+03 m^3).

Subcatchment	1979	1989	1999	2009	2017
S1	1816.86	3634.22	4055.24	4936.31	6050.33
S2	6663.67	10,929.96	17,061.33	24,903.05	35,397.17
S3	1343.81	1764.48	1885.19	2077.1	2190.72
S4	814.82	2509.89	4258.44	5390.18	7154.39
S5	15,410.19	20,969.34	25,488.93	29,758.98	31,885.98
S6	1781.52	2496.24	3103.26	4554.51	4789.84
S7	1023.74	1237.22	1287.62	1288.84	1291.21
S8	3984.18	5807.47	7288.18	10,892.26	13,671.31
S9	1593.02	1627.73	1669.24	1669.24	1667.82
S10	5086.38	6342.07	6397.92	6397.54	6372.08
S11	8293.31	11,427.18	12,210.24	12,909.56	13,021.93
S12	3528.44	5283.69	5857.24	5917.89	5928.5
S13	3165.02	4277.61	4408.38	4474.5	4489.58
S14	4726.05	7356.74	10,216.65	12,240.23	12,866.25
S15	4999.04	6810.62	8474.48	8937.21	8796.22
O1	65,986.71	94,584.40	116,017.50	138,918.79	158,203.80

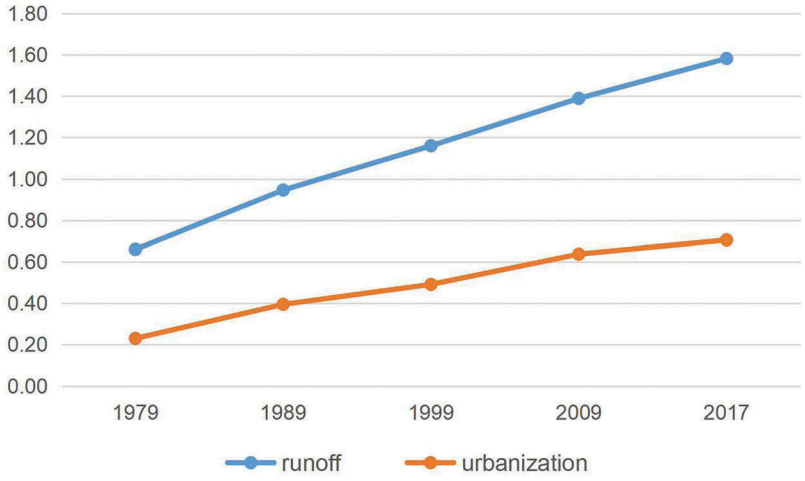

Figure 11. Comparison between urbanization rate and runoff change.

Table 5. Value of runoff coefficient calculated based on the simulated total runoff.

Subcatchment	1979	1989	1999	2009	2017
S1	0.084	0.168	0.187	0.228	0.279
S2	0.052	0.086	0.134	0.195	0.277
S3	0.093	0.123	0.131	0.144	0.152
S4	0.057	0.176	0.299	0.378	0.502
S5	0.159	0.216	0.263	0.307	0.329
S6	0.113	0.158	0.196	0.288	0.303
S7	0.39	0.472	0.491	0.491	0.492
S8	0.109	0.159	0.199	0.298	0.374
S9	0.452	0.462	0.474	0.474	0.473
S10	0.482	0.601	0.606	0.606	0.603
S11	0.273	0.376	0.402	0.425	0.428
S12	0.278	0.417	0.462	0.467	0.467
S13	0.345	0.466	0.481	0.488	0.49
S14	0.132	0.205	0.284	0.341	0.358
S15	0.296	0.403	0.502	0.529	0.521

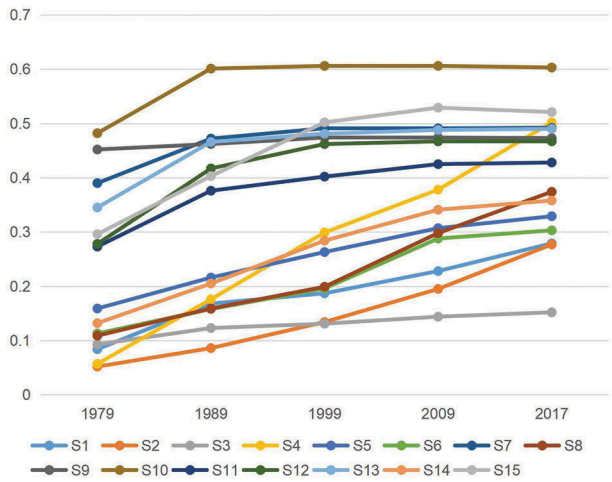

Figure 12. Runoff change in each subcatchment.

trend from 2009 to 2017. According to the investigation results, the rivers in those areas and adjacent areas were encountering heavy overflowing caused by the blocking of several illegal constructions and shanty cabins on the river, weakening the drainage capacity compared with the designed one. Those covers had been demolished later to restore the designed level. In addition, with paying much focus on the sustainable development, plenty of runoff regulation measures and green space might also make effects on the results. Figure 13 depicts the spatial variation of the runoff coefficient in each subcatchment in 1979, 1989, 1999, 2009 and 2017. It can be found that the change direction presents a Z-like from the south to the north then to the south again, which indirectly reflects the urban development process in the past 30 years in Jinan.

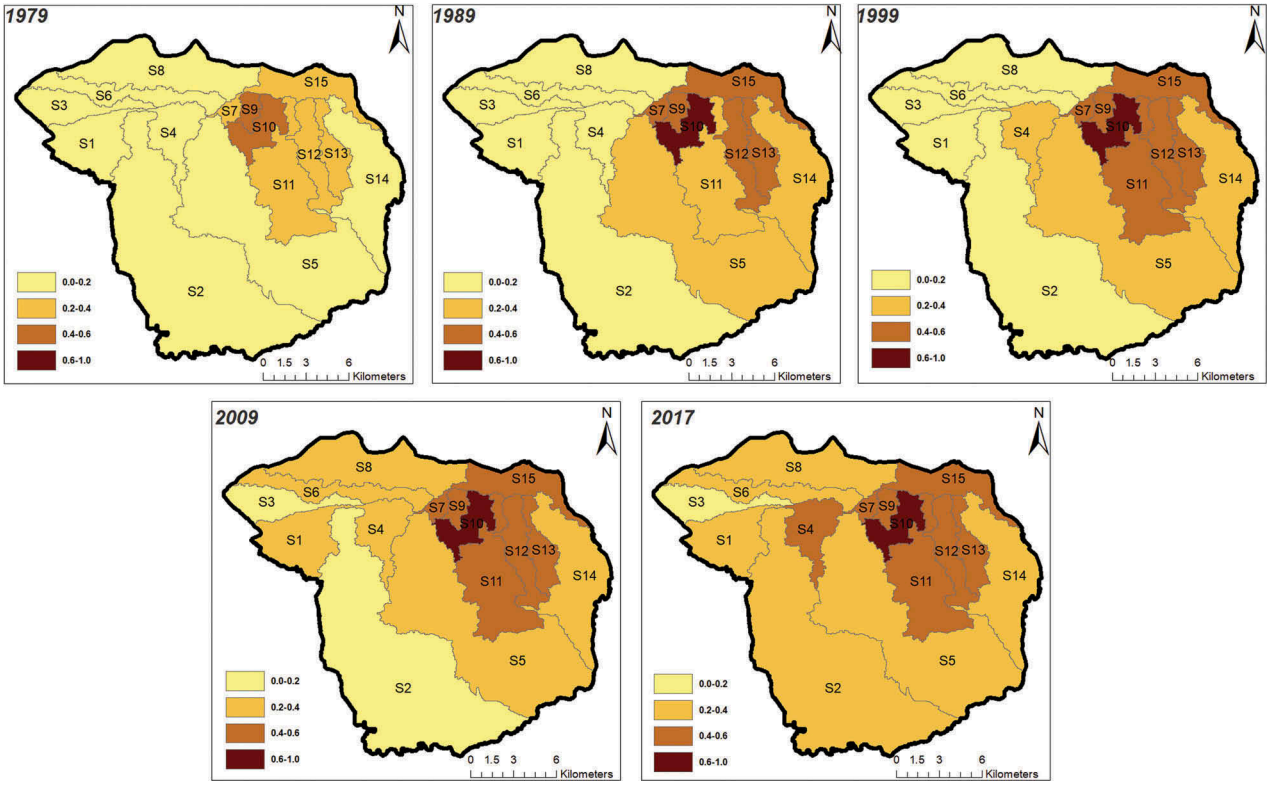

Figure 13. Spatial variation of the runoff coefficient in each subcatchment.

Effectiveness of the coupled LIDs

According to the characteristics of runoff changes in the study area, the coupled LIDs were deployed in the subcatchments whose runoff coefficients are greater than 0.4, as shown in Figure 14. Objects in SWMM used for representing LIDs were also created to simulate runoff response based on the base scenario and three coupled LIDs scenarios. We analyze and discuss the results in the next paragraphs.

Tables 6 and 7 respectively list the reduction percentage of the total runoff and the peak runoff of each subcatchment calculated in the base scenario and the coupled LIDs scenarios. It can be demonstrated that reduction quantity on the total runoff from the three scenarios is larger than on the peak runoff no matter in the individual subcatchment or the whole watershed. On the one hand, due to difference in regulation capacity of individual LIDs for the total runoff and peak runoff, the combination scheme responded an accumulation effect. On the other hand, it might also reveal that the effectiveness of the coupled LIDs for the low-intensity runoff regulation is superior to the high-intensity one. Besides, the decreased percentages both on the total runoff and the peak runoff in the subcatchments are greater than in the whole watershed. It might be because of a lack of LIDs in certain subcatchments, which results in less comprehensive impacts on the whole research area than on the subcatchments deployed with LIDs. Probably, the capacity of the coupled LIDs for regulating runoff could be weakened with the increase of the spatial scale. By comparing the decrease percentages of the total runoff and the peak runoff generated from those scenarios, we find that scenario 1 presents an improved effect on the controlling of the total runoff, while scenario 2 shows the best controlling effect on the peak runoff. Figure 15 intuitively depicts the results mentioned above of the coupled LIDs scenarios from the spatial scale.

We also estimated the costs of each proposed scenario for reducing one cubic meter of the total runoff based on the simulation results and the construction and maintenance costs of the individual LIDs in China. They are 14.23 yuan, 32.63 yuan, and 25.77 yuan for scenario 1, scenario 2 and scenario 3, respectively. Note that the costs of each individual LIDs depend on the local developing level.

Conclusion

As mentioned in previous sections, LIDs are initially designed to regulate or control runoff and non-point source pollution, belonging to the scope of urban storm or flooding management. Due to landscape values of certain LIDs and the new requirements that coupling them into urban planning and ecosystem protection in current urban development strategies, much extensional application and understanding have been carried out, such as the “Sponge City” in China. However, along with the increasing interests in the large area, the effectiveness data of LIDs from the

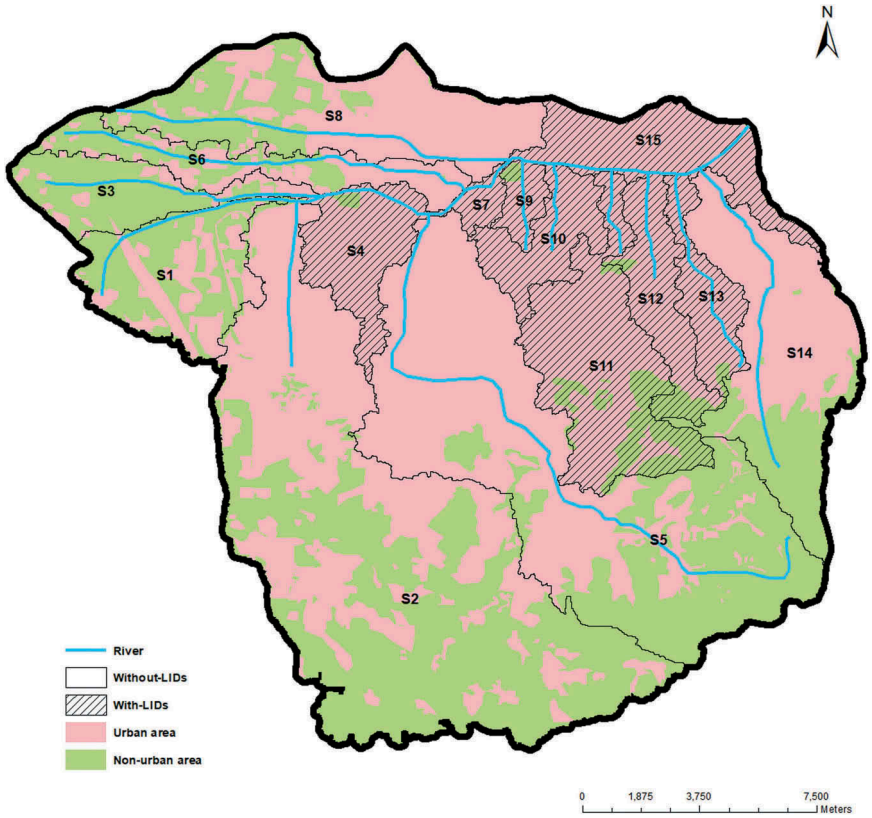

Figure 14. The deployment of the coupled LIDs in Huangtaiqiao watershed.

Table 6. Reduction percentage of the total runoff with the action of the coupled LIDs. (unit: million gal; 1 million gal = 3.7854e+03 m^3).

		Scenario 1		Scenario 2		Scenario 3	
Subcatchment	Base	Total runoff	Reduction percent	Total runoff	Reduction percent	Total runoff	Reduction percent
S4	7154.39	2607.89	63.55%	3169.52	55.70%	4234.35	40.81%
S7	1291.21	466.62	63.86%	551.47	57.29%	753.9	41.61%
S9	1667.82	577.05	65.40%	735.62	55.89%	972.46	41.69%
S10	6372.08	2653.48	58.36%	2771.96	56.50%	3844.14	39.67%
S11	13,021.93	3217.96	75.29%	4917.6	62.24%	7019.75	46.09%
S12	5928.5	1816.48	69.36%	2434.71	58.93%	3361.68	43.30%
S13	4489.58	1395.91	68.91%	1986.76	55.75%	2584.74	42.43%
S15	8796.22	3330.46	62.14%	3969.57	54.87%	5272.13	40.06%
O1	158,203.80	125,816.21	20.47%	130,352.97	17.60%	137,838.00	12.87%

Table 7. Reduction percentage of the peak runoff with the action of the coupled LIDs. (unit: ft^3/s; $1ft^3/s$ = 2.83168e-02 m^3/s).

		Scenario 1		Scenario 2		Scenario 3	
Subcatchment	Base	Peak runoff	Reduction percent	Peak runoff	Reduction percent	Peak runoff	Reduction percent
S4	1224.79	1083.31	11.55%	921.73	24.74%	1093.9	10.69%
S7	228.60	211.39	7.53%	181.84	20.45%	214.2	6.30%
S9	296.18	277.87	6.18%	243.37	17.83%	281.65	4.91%
S10	1033.54	909.08	12.04%	763.13	26.16%	934.08	9.62%
S11	2583.98	2203.96	14.71%	1877.65	27.33%	2287.99	11.45%
S12	1283.15	1153.54	10.10%	998.42	22.19%	1172.49	8.62%
S13	964.46	893.26	7.38%	793.27	17.75%	903.18	6.35%
S15	1542.92	1399.12	9.32%	1227.74	20.43%	1410.18	8.60%
O1	21,268.42	21,146.60	0.57%	20,956.50	1.47%	21,154.44	0.54%

micro-scale on-site tests or experiments based on the conventional monitoring means would be not enough because of those limitations demonstrated in the first section of this paper. Therefore, to enrich the application scale and surmount the limitations, we evaluated the effectiveness of the coupled LIDs system from the watershed scale with several mixed LULC based on remote sensing image processing, scenario designation and SWMM simulation. The results show that the controlling efficiency of the coupled LIDs for the total runoff is superior for the peak runoff. The coupled system of rain tanks, rain gardens and permeable paving presents better effect on subcatchments compared with the whole watershed. Namely, with

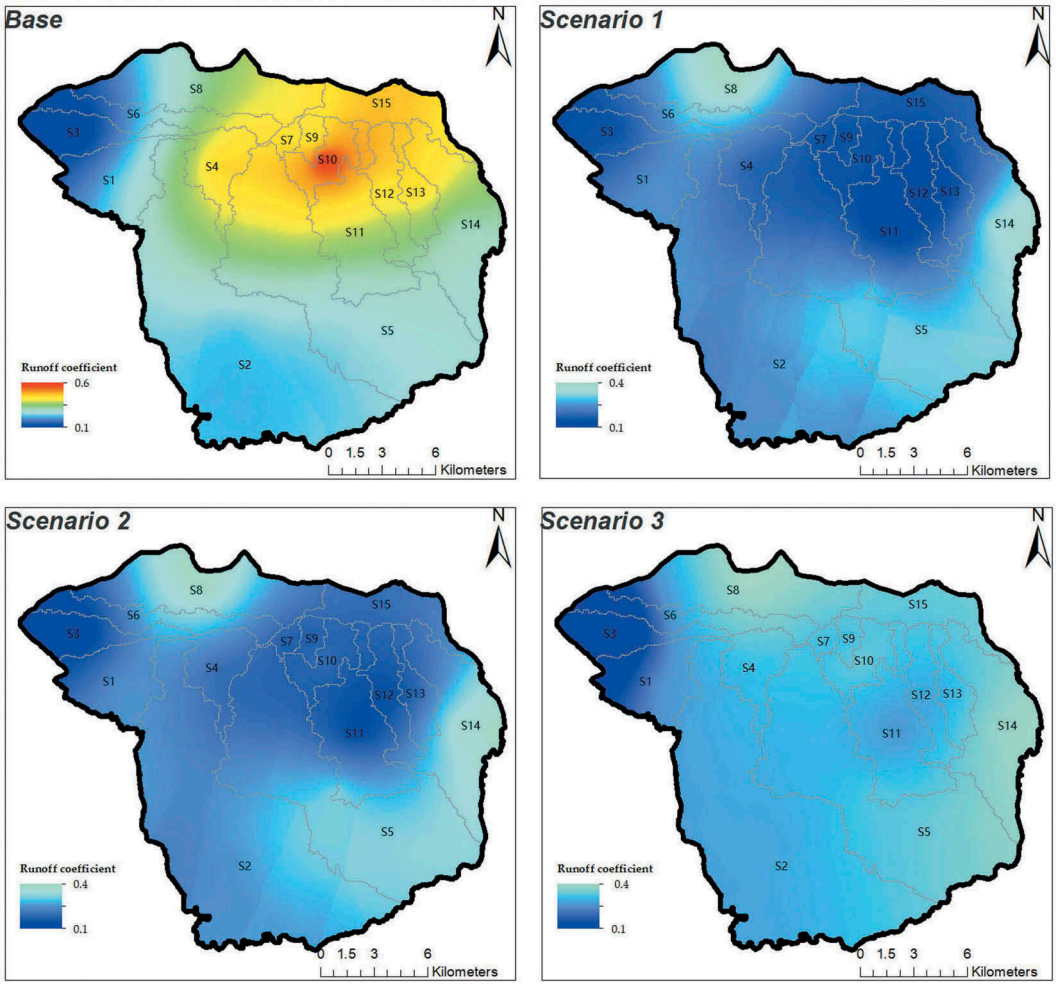

Figure 15. Runoff response to the coupled LIDs scenarios.

the increase of the spatial scale, the effectiveness appears to present a decreasing trend. In addition, we estimated the costs of each proposed scenario, and the economic benefit of scenario 1, scenario 3 and scenario 2 reduces in order, which could be used for decision supporting of the urban designers and urban planners. The results also prove that the coupled LIDs are more effective than the individual used LIDs. As the inheriting links, the characteristics of LULC change and the runoff change in urban area of Jinan were also analyzed and discussed, which would be beneficial to the local urban planning and on-going construction of the "Sponge City". Besides, our research indirectly verified the expected benefit of hydrological features as a significant indicator to measure the urbanization level. As recommendation in the end, for the general understanding of the coupled LIDs effectiveness, more research focusing on the type and the coupled structure of various LIDs should be launched in the future.

Disclosure statement

No potential conflict of interest was reported by the authors.

References

Ahiablame, L. M., Engel, B. A., & Chaubey, I. (2012). Effectiveness of low impact development practices: Literature review and suggestions for future research. *Water, Air, and Soil Pollution*, *223*(7), 4253–4273. https://doi.org/10.1007/s11270-012-1189-2

Al Maimuri, N. M. L. (2018). Applicability of Horton model and recharge evaluation in irrigated arid Mesopotamian soils of Hashimiya, Iraq. *Arabian Journal of Geosciences*, *11*(20). https://doi.org/10.1007/s12517-018-3986-4

Altenau, E. H., Pavelsky, T. M., Moller, D., Pitcher, L. H., Bates, P. D., Durand, M. T., & Smith, L. C. (2019). Temporal variations in river water surface elevation and slope captured by AirSWOT. *Remote Sensing of Environment*, *224*, 304–316. https://doi.org/10.1016/j.rse.2019.02.002

Campisano, A., Catania, F. V., & Modica, C. (2016). Evaluating the SWMM LID editor rain barrel option for the estimation of retention potential of rainwater harvesting systems. *Urban Water Journal*, *14*(8), 876–881. https://doi.org/10.1080/1573062x.2016.1254259

Ding, L., Ren, X., Gu, R., & Che, Y. (2019). Implementation of the "Sponge City" development plan in China: An evaluation of public willingness to pay for the life-cycle maintenance of its facilities. *Cities*, *93*, 13–30. https://doi.org/10.1016/j.cities.2019.04.007

Eckart, K., McPhee, Z., & Bolisetti, T. (2017). Performance and implementation of low impact development - a

review. *Science of the Total Environment*, *607–608*, 413–432. https://doi.org/10.1016/j.scitotenv.2017.06.254

Eckle, K., & Schmidt-Hieber, J. (2018). A comparison of deep networks with ReLU activation function and linear spline-type methods. *Neural Networks*, *110*, 232–242. https://doi.org/10.1016/j.neunet.2018.11.005

Fu, Q., Hu, C., Peng, J., & Yue, S. (2018). Shaping the collision selectivity in a looming sensitive neuron model with parallel ON and OFF pathways and spike frequency adaptation. *Neural Networks*, *106*, 127–143. https://doi.org/10.1016/j.neunet.2018.04.001

Ghorbanzadeh, O., Blaschke, T., Gholamnia, K., Meena, S., Tiede, D., & Aryal, J. (2019). Evaluation of different machine learning methods and deep-learning convolutional neural networks for landslide detection. *Remote Sensing*, *11*(2), 196. https://doi.org/10.3390/rs11020196

Gilbreath, A., McKee, L., Shimabuku, I., Lin, D., Werbowski, L. M., Zhu, X., & Rochman, C. (2019). Multiyear water quality performance and mass accumulation of PCBs, Mercury, Methylmercury, Copper, and Microplastics in a bioretention rain garden. *Journal of Sustainable Water in the Built Environment*, *5*(4), 04019004. https://doi.org/10.1061/jswbay.0000883

Gisvold, J. B., Hamouz, V., Seifu, G. A., & Merete, M. T. (2019). The transferability of SWMM model parameters between green roofs with similar build-up. *Journal of Hydrology*, *569*, 816–828. https://doi.org/10.1016/j.jhydrol.2019.01.004

Gu, C., Cockerill, K., Anderson, W. P., Shepherd, F., Groothuis, P. A., Mohr, T. M., & Zhang, C. (2019). Modeling effects of low impact development on road salt transport at watershed scale. *Journal of Hydrology*, *574*, 1164–1175. https://doi.org/10.1016/j.jhydrol.2019.04.079

Guo, X., Guo, Q., Zhou, Z., Du, P., & Zhao, D. (2019). Degrees of hydrologic restoration by low impact development practices under different runoff volume capture goals. *Journal of Hydrology*, *578*, 124069. https://doi.org/10.1016/j.jhydrol.2019.124069

Hao, M., Gao, C., Sheng, D., & Qing, D. (2019). Review of the influence of low-impact development practices on mitigation of flood and pollutants in urban areas. *Desalination and Water Treatment*, *149*, 323–328. https://doi.org/10.5004/dwt.2019.23852

He, B., Zhu, J., Zhao, D., Gou, Z., Qi, J., & Wang, J. (2019). Co-benefits approach: Opportunities for implementing Sponge City and urban heat island mitigation. *Land Use Policy*, *86*, 147–157. https://doi.org/10.1016/j.landusepol.2019.05.003

Hou, J., Zhang, Y., Tong, Y., Guo, K., Qi, W., & Hinkelmann, R. (2019). Experimental study for effects of terrain features and rainfall intensity on infiltration rate of modelled permeable pavement. *Journal of Environmental Management*, *243*, 177–186. https://doi.org/10.1016/j.jenvman.2019.04.096

Jain, G. V., Agrawal, R., Bhanderi, R. J., Jayaprasad, P., Patel, J. N., Agnihotri, P. G., & Samtani, B. M. (2015). Estimation of sub-catchment area parameters for Storm Water Management Model (SWMM) using geo-informatics. *Geocarto International*, *31*(4), 462–476. https://doi.org/10.1080/10106049.2015.1054443

Jinan Bureau of Statistics. (2019). *Statistical yearbook of Jinan in 2018*. China Statistics Press.

Jinan Municipal People's Government. (2019, April 17). *Statistical bulletin of national economic and social development of Jinan in 2018*. http://www.jinan.gov.cn/art/2019/4/17/art_3503_2902947.html?xxgkhide=1

Ketabchy, M., Sample, D. J., Wynn-Thompson, T., & Yazdi, M. N. (2019). Simulation of watershed-scale practices for mitigating stream thermal pollution due to urbanization. *Science of the Total Environment*, *671*, 215–231. https://doi.org/10.1016/j.scitotenv.2019.03.248

Kim, J., & Joo, J. (2018). Evaluation of low impact development using EPA SWMM-LID modeling. *International Conference on Hydroinformatics*, *3*, 1078–1080. https://doi.org/10.29007/k8gk

Ma, L., Liu, Y., Zhang, X., Ye, Y., Yin, G., & Johnson, B. A. (2019). Deep learning in remote sensing applications: A meta-analysis and review. *ISPRS Journal of Photogrammetry and Remote Sensing*, *152*, 166–177. https://doi.org/10.1016/j.isprsjprs.2019.04.015

Noh, S., Chung, E. S., & Seo, Y. (2015). Performance of a rain barrel sharing network under climate change. *Water*, *7*(12), 3466–3485. https://doi.org/10.3390/w7073466

Oosterbaan, R. J. (2019). Rainfall-runoff relations of a small valley assessed with a Non-linear reservoir model. *International Journal of Environmental Science*, *4*, 20–27. https://www.iaras.org/iaras/home/caijes/rainfall-runoff-relations-of-a-small-valley-assessed-with-a-non-linear-reservoir-model

Pham, T. D., Yokoya, N., Bui, D. T., Yoshino, K. A., & Friess, D. (2019). Remote sensing approaches for monitoring mangrove species, structure, and biomass: Opportunities and challenges. *Remote Sensing*, *11*(3), 230. https://doi.org/10.3390/rs11030230

Shafique, M., Kim, R., & Kyung-Ho, K. (2018). Evaluating the capability of grass swale for the rainfall runoff reduction from an urban parking lot, Seoul, Korea. *International Journal of Environmental Research and Public Health*, *15*(3), 537. https://doi.org/10.3390/ijerph15030537

Shen, C. (2018). A trans-disciplinary review of deep learning research and its relevance for water resources scientists. *Water Resources Research*, *54*(11), 8558–8593. https://doi.org/10.1029/2018wr022643

Thakali, R., Qaiser, K., Kalra, A., & Ahmad, S. (2018). Management of an urban stormwater system using projected future scenarios of climate models: A watershed-based modeling approach. *Open Water Journal*, *5(2)*, 1–15. https://scholarsarchive.byu.edu/openwater/vol5/iss2/1

Tuomela, C., Sillanpää, N., & Koivusalo, H. (2018). Assessment of stormwater pollutant loads and source area contributions with storm water management model (SWMM). *Journal of Environmental Management*, *233*, 719–727. https://doi.org/10.1016/j.jenvman.2018.12.061

Wang, H., Mei, C., Liu, J., & Shao, W. (2018). A new strategy for integrated urban water management in China: Sponge City. *Science China Technological Sciences*, *61*(3), 317–329. https://doi.org/10.1007/s11431-017-9170-5

Wang, J., Che, W., & Yi, H. (2010). Research and progress of stormwater management models based on low-impact development. *China Water & Wastewater*, *26*(18), 50–54. http://en.cnki.com.cn/Article_en/CJFDTotal-GSPS201018014.htm

Wang, J., Wang, Y., & Ye, T. (2004). Urban flood risk and sustainable development in China. *Journal of Beijing Normal University*, *3*, 138–143. http://www.cnki.com.cn/Article/CJFDTotal-BJSF200403020.htm

Wang, M., Zhang, D., Su, J., Dong, J., & Tan, S. (2018). Assessing hydrological effects and performance of low impact development practices based on future scenarios

modeling. *Journal of Cleaner Production*, *179*, 12–23. https://doi.org/10.1016/j.jclepro.2018.01.096

Xia, J., Zhang, Y., Xiong, L., He, S., Wang, L., & Yu, Z. (2017). Opportunities and challenges of the Sponge City construction related to urban water issues in China. *Science China Earth Sciences*, *60*(4), 652–658. https://doi.org/10.1007/s11430-016-0111-8

Xu, T., Li, K., Engel, B. A., Jia, H., Leng, L., Sun, Z., & Yu, S. (2019). Optimal adaptation pathway for sustainable low impact development planning under deep uncertainty of climate change: A greedy strategy. *Journal of Environmental Management*, *248*, 109280. https://doi.org/10.1016/j.jenvman.2019.109280

Yu, K., Li, D., Yuan, H., Fu, W., Qiao, Q., & Wang, S. (2015). "Sponge City": Theory and practice. *City Planning Review*, *39*(6), 26–36. http://en.cnki.com.cn/Article_en/CJFDTotal-CSGH201506009.htm

Zhao, C., Yang, Y., Yang, S., Gai, Y., Zhang, C., Zhang, H., & Zhang, Z. (2019). Factors driving temporospatial heterogeneity of fish community health in Jinan City, China. *Marine & Freshwater Research*, *70*(5), 637. https://doi.org/10.1071/mf18337

Zhao, M., Cheng, W., Zhou, C., Li, M., Huang, K., & Wang, N. (2019). Assessing spatiotemporal characteristics of urbanization dynamics in southeast Asia using time series of DMSP/OLS nighttime light data. *Remote Sensing*, *10*(2), 47. https://doi.org/10.3390/rs10010047

Zhao, Y., Xu, Z., Zhao, G., Cheng, X., & Tan, Q. (2019). Impact of urbanization on regional rainfall-runoff processes in Xiaoqing River basin, Jinan. *Journal of Hydroelectric Engineering*, *38*(10), 35–46. http://www.cnki.com.cn/Article/CJFDTotal-SFXB201910004.htm